Mechanism, kinetics and modelling of inverse-microsuspension polymerization: 2. Copolymerization of acrylamide with quaternary ammonium cationic monomers

D. Hunkeler and A. E. Hamielec
Institute for Polymer Production Technology, Department of Chemical Engineering, McMaster University, Hamilton, Ontario, Canada L8S 4L7
(Received 11 April 1990; accepted 30 June 1990)

A mechanism has been developed for the inverse-microsuspension polymerization of acrylic water-soluble monomers. This includes the influence of ionogenic monomers and polyelectrolytes, and has been applied to the copolymerization of acrylamide with quaternary ammonium species. A multistage experimental investigation has also been conducted so that phenomena unique to the kinetic model can be isolated, and independent parameter estimates generated. This included: homopolymerizations in aqueous solution and inverse microsuspension, to measure the rate parameter $k_p/k_t^{1/2}$ and decouple it from the initiation efficiency; monomer partitioning measurements to distinguish the rate of macroradical chain addition in the aqueous and organic phases; and copolymerization in inverse microsuspension. The reaction system consisted of the cationic monomers dimethylaminoethyl acrylate and dimethylaminoethyl methacrylate, Isopar-K as the organic phase, and fatty acid esters of sorbitan as steric stabilizers. Polymerizations were performed between 40 and 60°C and were chemically initiated with oil-soluble (azobisisobutyronitrile) and water-soluble (potassium persulphate) species. These experiments have confirmed the three main postulates of the reaction mechanism: specifically, that nucleation and polymerization occur within the monomer droplets; heterophase diffusion-limited oligoradical precipitation is the predominant initiation reaction; and unimolecular termination with interfacial species is competitive with the bimolecular process. Further, propagation and termination were not found to be influenced by the nature of the polymerization system, proceeding at equal rates in solution and inverse microsuspension. The kinetic model is therefore found to be in excellent agreement with experimental polymerization rate, copolymer composition and particle size data.

(Keywords: inverse microsuspension; inverse emulsion; acrylamide; water-soluble polymers; dimethylaminoethyl acrylate; dimethylaminoethyl methacrylate)

INTRODUCTION

Over the past two decades the commercial use of cationic water-soluble polymers has increased rapidly. Cationic homopolymers and copolymers with acrylamide are now applied as retention aids in paper making[1], as flocculants and biocides in water treatment[2,3], as dispersants[4], as stabilizers for emulsion polymerization[5–7], in cosmetics and pharmaceuticals[8,9] and in general wherever aqueous solid–liquid separations are required.

Cationic polymers can be categorized by the chemical nature of the charged substituent. Ammoniums (primary, secondary, tertiary and quaternary) have had the most significant commercial impact, since they can be synthesized to a variety of chain architectures and sizes. By comparison, polyphosphoniums are limited to oligomeric molecular weights[10–13], and sulphonium monomers are generally unstable and less readily available than quaternary ammonium compounds[14,15].

Ammonium-containing polymers were first synthesized by Marvel[16] in 1930. However, it was not until 1949 that quaternized macromolecules were produced[17]. In that investigation, tri- and tetraallylammonium salts were polymerized to form highly crosslinked ion-exchange resins. In 1951, Butler and Ingley[18] reported the formation of a water-soluble polymer from diallyl quaternary bromides*. Later Butler[19] showed that the chloride ion form of diallylammonium monomers provided more useful products owing to their higher molecular weights. The solubility of diallyl monomers was surprising, since at the time it was believed that all dienes yielded crosslinked gels[20]. To account for this phenomenon, Butler and Angelo[21] proposed an alternating inter–intramolecular chain propagation. 'Cyclopolymerization' occurs because the ring formation is kinetically more favourable than a second intermolecular linkage. Wandrey[22] has determined that ring closure accounts for up to 99.9% of addition reactions, with the remaining forming pendant double bonds. Butler and Angelo's mechanism included a radical attack on the α-carbon followed by cyclization to the α-carbon of the residual double bond.

Over the past 30 years research in cyclopolymerization has grown rapidly. Almost all non-conjugated dienes are now believed to undergo cyclic formation in competition with, and often in preference to, crosslinking. Suitable

* The apparent unreactivity of monoallyl compounds is due to a strong depropagation reaction

0032-3861/91/142626-15

monomers can be initiated by a number of mechanisms including free-radical, anionic and cationic processes[23].

The elucidation of the mechanism of ring closure has propelled cyclopolymerization from the status of a novel polymerization technique to the forefront of theoretical free-radical chemistry. Originally a six-member ring structure was postulated, since it can be obtained via a secondary radical intermediate that is thermodynamically more favourable than the reaction pathway required for five-member rings. However, Brace[24,25] investigated the free-radical addition of perfluoroallyl radicals to N-substituted diallylamines and observed exclusively five-member ring formation. ^{13}C nuclear magnetic resonance studies of diallyldimethylammonium chloride and bromide have also failed to detect six-member rings[26,27]. Electron spin resonance investigations have supported these findings[28].

Ottenbrite and Shillady[27] have applied molecular orbital theory to show that the approach of a radical to a β-carbon is less sterically hindered, implying that monocyclic reactions are kinetically controlled and, for diallylammoniums, produce pyrrolidinium rings in preference to piperidinium rings. In general, five-member ring formation is energetically more favourable unless the β-carbon contains large substituents, which interfere with its approach to the radical[28].

Poly(diallyldimethylammonium chloride) (PDADMAC) was the first synthetic flocculant approved for potable water clarification by the United States Public Health Service[29], and has historically been the most widely produced polyelectrolyte. Other commercially important cationic polymers are derived from dimethylaminoethyl methacrylate (DMAEM), first synthesized by Winberg[30] in 1956, dimethylaminoethyl acrylate (DMAEA) and acrylamidomethylpropanedimethylammonium chloride (AMPDAC). These cationic monomers are often copolymerized with acrylamide to produce supermolecular polyelectrolyte structures. The resulting flocculants are non-toxic and more efficient than either of the respective non-ionic and cationic homopolymers[31]. They also offer advantages over inorganic flocculants such as alum, including smaller dosage requirements, less floc generation and a reduction of the ash produced during incineration. As such, synthetic polyelectrolytes have occupied a growing portion of the water treatment market over the past two decades.

Kinetics

Kinetic investigations of the polymerization of quaternary ammonium monomers are limited to observations on dimethylamines and diallylammoniums. For DMAEM, Longi[32], Egoyan[33–35], Martynenko[36] and Fujimori[37] have conducted polymerizations in solvents with various polarity and found conformation to the classical free-radical polymerization mechanism. However, investigations with DADMAC[38–42] have revealed two kinetic anomalies: a linear dependence of the propagation rate constant on monomer concentration[22,43] and the formation of a molecular complex with anionic peroxide initiators[44,45]. The former is caused by an increase in the electrolyte level of the mixture with added monomer, which suppresses Coulombic interactions and increases the reactivity of charged monomers and macroradicals. The latter is due to the ionogenic nature of the monomer and initiator, and has been mechanistically described by Hunkeler[46].

Investigations of the copolymerization kinetics are also limited even though acrylamide (AAM) and quaternary ammoniums were first reacted in 1959[1]. Hunkeler[47] has recently published an extensive study of the copolymerization of acrylamide with DMAEA, DMAEM and DADMAC. This combined the statistically precise error-in-variables parameter estimation method with h.p.l.c. measurements of the residual monomer concentrations. The latter was found to have a sensitivity below 1 ppm with a reproducibility of $\pm 0.25\%$. This showed considerable improvements over the colloid titration methods that have been previously employed[48–50]. Further, the error-in-variables method provided the means for estimating the joint confidence region for the reactivity ratios, the area of which is proportional to the total measurement error. The reactivity ratios and their 95% confidence intervals are summarized in *Table 1*. *Table 2* compares Hunkeler's reactivity ratios for AAM/DADMAC with those determined previously. Good agreement is observed with the results of Wandrey[52]. A linear dependence of DADMAC reactivity ratio with the simple electrolyte concentration has also been reported[53].

The reactivity of quaternary ammonium monomers has been determined to be insensitive to the pH of the reaction mixture[50] and the size of the substituents on the ammonium groups[54]. However, functional groups closer to the reactive centre can have an appreciable influence on the rate and molecular size, with monomers with ester linkages polymerizing faster than their amino counterparts[55].

Inverse-microsuspension polymerization

Inverse microsuspension is a heterogeneous water-in-oil polymerization process, used for the synthesis of

Table 1 Reactivity ratios of the polymerization of acrylamide (AAM) with different cationic monomers under various conditions

Monomer system	r_1 (AAM)	r_2 (Cationic)	Initiator[a]	Temperature (°C)
AAM/DMAEM[b]	0.49 ± 0.15	2.46 ± 0.40	ACV	60
AAM/DMAEM	0.61 ± 0.07	2.52 ± 0.19	KPS	60
AAM/DMAEM[b]	0.43 ± 0.18	2.39 ± 0.38	ACV	45
AAM/DMAEA[c]	0.29 ± 0.07	0.34 ± 0.09	ACV	60
AAM/DMAEA[c]	0.33 ± 0.09	0.40 ± 0.11	ACV	45
AAM/DADMAC	6.4 ± 0.4	0.06 ± 0.03	ACV	50

[a] ACV = azocyanovaleric acid; KPS = potassium persulphate
[b] $r_1 = 7.823 \exp(-923/T)$, $r_2 = 4.538 \exp(-204/T)$
[c] $r_1 = 1.871 \times 10^{-2} \exp(913/T)$, $r_2 = 1.083 \times 10^{-2} \exp(1148/T)$

Table 2 Comparison of the reactivity ratios determined by different authors for the copolymerization of AAM with DADMAC

r_1	r_2	Monomer concentration (mol l^{-1})	Temperature (°C)	Range of feed ratios, f_1	Reference
6.4 ± 0.4	0.06 ± 0.03	0.5	50	$0.3 \rightarrow 0.7$	This work
6.7	0.58	1.5	20	$0.1 \rightarrow 0.9$	Tanaka[50]
6.62[a]	0.074[a]	3.0	35	$0.11 \rightarrow 0.89$	Wandrey[52]
7.14[a]	0.22[a]	4.0	35	$0.2 \rightarrow 0.72$	Wandrey[52]
7.54[b]	0.049[b]	5.75	47	$0.2 \rightarrow 0.8$	Huang[51]

[a]These are average values, since r_1 and r_2 were observed to depend on the feed ratio
[b]Determined in inverse-emulsion polymerization

high-molecular-weight acrylic water-soluble polymers. These 'inverse macroemulsions' are thermodynamically unstable, turbid, inviscid and possess excellent heat transfer characteristics, particularly at high monomer concentrations. Further, they can be used to prepare directly dilute aqueous polymer solutions, needed for commercial applications, by inverting in an excess of water. Inverse microsuspensions therefore overcome the principal disadvantages of solution polymerization processes: inefficient reactor utilization through low monomer loadings, and gel blocking of the dried polymer.

Inverse microsuspensions are prepared by dispersing an aqueous monomer solution in an organic continuous phase, either aliphatic or aromatic. The emulsification is maintained through the addition of low HLB (hydrophilic–lyophilic balance) steric stabilizers and continuous, vigorous agitation. Small-molecule co-surfactants also have utility in creating a rigid interface and preventing coalescence. The polymerizations are usually chemically initiated with oil-soluble[56–60] or water-soluble[61,62] species. The former is more common.

In inverse microsuspension, nucleation and polymerization are confined to the aqueous monomer droplets, with each dispersed particle behaving as a segregated solution polymerization reactor (particle sizes are nominally 1–10 μm in diameter). The polymerization follows a free-radical mechanism with two additional elementary reactions: a heterophase mass-transfer-limited oligoradical precipitation, and unimolecular macroradical termination with interfacial species. The latter proceeds in competition with and often in preference to the conventional bimolecular process, and is manifested as a first-order rate dependence on initiator concentration.

Hunkeler[56] has developed a mechanism for the inverse-microsuspension homopolymerization of acrylamide in paraffinic media stabilized with fatty acid esters of sorbitan. The corresponding kinetic model has been found to provide excellent predictability of the polymerization rate, molecular weight and particle characteristics over a broad range of experimental conditions. In the following section of this paper, the mechanism will be generalized to copolymerizations. It will subsequently be evaluated against kinetic data for the polymerization of acrylamide with quaternary ammonium cationic comonomers.

MECHANISM

The mechanism derived for homopolymers[56] can easily be extended to copolymerizations by considering the unique reactivities of two monomers and two types of macroradicals; the latter distinguished by the composition of the terminal chain unit. For the notation used in this paper, subscript 1 denotes acrylamide and 2 the cationic comonomer.

Oil-phase reactions

Initiation

$$\mathrm{I} \xrightarrow{k_d} 2\mathrm{R}^{\bullet}_{\mathrm{in,o}} \tag{1}$$

where I denotes an initiator molecule and $\mathrm{R}^{\bullet}_{\mathrm{in}}$ a primary radical; and the subscript 'o' designates an oil-phase species.

Reactions of primary radicals

$$\mathrm{R}^{\bullet}_{\mathrm{in,o}} + \mathrm{HC} \xrightarrow{k_1} \text{Inert products} \tag{2}$$

$$\mathrm{R}^{\bullet}_{\mathrm{in,o}} + \mathrm{E} \xrightarrow{k_2} \text{Inert products} \tag{3}$$

$$\mathrm{R}^{\bullet}_{\mathrm{in,o}} + \mathrm{M}_{1,\mathrm{o}} \xrightarrow{k_{p1}} \mathrm{R}^{\bullet}_{1,1,\mathrm{o}} \tag{4}$$

$$\mathrm{R}^{\bullet}_{\mathrm{in,o}} + \mathrm{M}_{2,\mathrm{o}} \xrightarrow{k_{p2}} \mathrm{R}^{\bullet}_{1,2,\mathrm{o}} \tag{5}$$

where $\mathrm{R}^{\bullet}_{i,j}$ is the radical of length i with an end unit of type j ($j = 1, 2$); and HC, E and M denote hydrocarbon, emulsifier and monomeric species, respectively.

Propagation

$$\mathrm{R}^{\bullet}_{r,1,\mathrm{o}} + \mathrm{M}_{1,\mathrm{o}} \xrightarrow{k_{p11}} \mathrm{R}^{\bullet}_{r+1,1,\mathrm{o}} \tag{6}$$

$$\mathrm{R}^{\bullet}_{r,1,\mathrm{o}} + \mathrm{M}_{2,\mathrm{o}} \xrightarrow{k_{p12}} \mathrm{R}^{\bullet}_{r+1,2,\mathrm{o}} \tag{7}$$

$$\mathrm{R}^{\bullet}_{r,2,\mathrm{o}} + \mathrm{M}_{1,\mathrm{o}} \xrightarrow{k_{p21}} \mathrm{R}^{\bullet}_{r+1,1,\mathrm{o}} \tag{8}$$

$$\mathrm{R}^{\bullet}_{r,2,\mathrm{o}} + \mathrm{M}_{2,\mathrm{o}} \xrightarrow{k_{p22}} \mathrm{R}^{\bullet}_{r+1,2,\mathrm{o}} \tag{9}$$

Transfer between phases

$$\mathrm{M}_{1,\mathrm{o}} \overset{\Phi_{m1}}{\rightleftharpoons} \mathrm{M}_{1,\mathrm{w}} \tag{10}$$

$$\mathrm{M}_{2,\mathrm{o}} \overset{\Phi_{m2}}{\rightleftharpoons} \mathrm{M}_{2,\mathrm{w}} \tag{11}$$

$$\mathrm{R}^{\bullet}_{\mathrm{in,o}} \xrightarrow{k_r} \mathrm{R}^{\bullet}_{\mathrm{in,w}} \tag{12}$$

$$\mathrm{R}^{\bullet}_{r,1,\mathrm{o}} \xrightarrow{k_{r,r,1}} \mathrm{R}^{\bullet}_{r,1,\mathrm{w}} \tag{13}$$

$$\mathrm{R}^{\bullet}_{r,2,\mathrm{o}} \xrightarrow{k_{r,r,2}} \mathrm{R}^{\bullet}_{r,2,\mathrm{w}} \tag{14}$$

where the subscript 'w' denotes a water-phase species; and $k_{r,i,j}$ is the mass-transfer constant between the organic and aqueous phases for a macroradical of length i with terminal mono group j.

Aqueous-phase reactions

Reactions of primary radicals

$$R^{\bullet}_{in,w} + M_{1,w} \xrightarrow{k_{p1}} R^{\bullet}_{1,1,w} \quad (15)$$

$$R^{\bullet}_{in,w} + M_{2,w} \xrightarrow{k_{p2}} R^{\bullet}_{1,2,w} \quad (16)$$

Propagation

$$R^{\bullet}_{r,1,w} + M_{1,w} \xrightarrow{k_{p11}} R^{\bullet}_{r+1,1,w} \quad (17)$$

$$R^{\bullet}_{r,1,w} + M_{2,w} \xrightarrow{k_{p12}} R^{\bullet}_{r+1,2,w} \quad (18)$$

$$R^{\bullet}_{r,2,w} + M_{1,w} \xrightarrow{k_{p21}} R^{\bullet}_{r+1,1,w} \quad (19)$$

$$R^{\bullet}_{r,2,w} + M_{2,w} \xrightarrow{k_{p22}} R^{\bullet}_{r+1,2,w} \quad (20)$$

$$''R^{\bullet}_{r,1,w} + M_{1,w} \xrightarrow{k_{p11}} ''R^{\bullet}_{r+1,1,w} \quad (21)$$

$$''R^{\bullet}_{r,1,w} + M_{2,w} \xrightarrow{k_{p12}} ''R^{\bullet}_{r+1,2,w} \quad (22)$$

$$''R^{\bullet}_{r,2,w} + M_{1,w} \xrightarrow{k_{p21}} ''R^{\bullet}_{r+1,1,w} \quad (23)$$

$$''R^{\bullet}_{r,2,w} + M_{2,w} \xrightarrow{k_{p22}} ''R^{\bullet}_{r+1,2,w} \quad (24)$$

where $''R^{\bullet}$ denotes a macroradical with a terminally unsaturated hydrocarbon, formed through monomolecular termination with interfacial species (steps (25) to (30)).

Unimolecular termination with interfacial emulsifier

$$R^{\bullet}_{r,1,w} + \Gamma_E \xrightarrow{k_{fE}} P_r + E^{\bullet} \quad (25)$$

$$''R^{\bullet}_{r,1,w} + \Gamma_E \xrightarrow{k_{fE}} ''P_r + E^{\bullet} \quad (26)$$

$$R^{\bullet}_{r,2,w} + \Gamma_E \xrightarrow{k_{fE2}} P_r + E^{\bullet} \quad (27)$$

$$''R^{\bullet}_{r,2,w} + \Gamma_E \xrightarrow{k_{fE2}} ''P_r + E^{\bullet} \quad (28)$$

where Γ_E denotes interfacial emulsifier; $E^{\bullet}$ is an emulsifier radical; P_r is a dead polymer chain of length r; the superscript $''$ designates terminal unsaturation; and steps (26) and (28) are negligible since at any instant in the reaction $[''R^{\bullet}] \ll [R^{\bullet}]$[56].

Reactions of emulsifier radicals

$$E^{\bullet} + M_{1,w} \xrightarrow{k_{p1}} ''R^{\bullet}_{1,1,w} \quad (29)$$

$$E^{\bullet} + M_{2,w} \xrightarrow{k_{p2}} ''R^{\bullet}_{1,2,w} \quad (30)$$

$$E^{\bullet} + HC_{imp} \xrightarrow{k_s} \text{Inert products} \quad (31)$$

where HC_{imp} designates hydrocarbon phase impurities or radical scavengers.

Transfer to monomer

$$R^{\bullet}_{r,1,w} + M_{1,w} \xrightarrow{k_{fm11}} P_r + R^{\bullet}_{1,w} \quad (32)$$

$$''R^{\bullet}_{r,1,w} + M_{1,w} \xrightarrow{k_{fm11}} ''P_r + R^{\bullet}_{1,w} \quad (33)$$

$$R^{\bullet}_{r,1,w} + M_{2,w} \xrightarrow{k_{fm12}} P_r + R^{\bullet}_{2,w} \quad (34)$$

$$''R^{\bullet}_{r,1,w} + M_{2,w} \xrightarrow{k_{fm12}} ''P_r + R^{\bullet}_{2,w} \quad (35)$$

$$R^{\bullet}_{r,2,w} + M_{1,w} \xrightarrow{k_{fm21}} P_r + R^{\bullet}_{1,w} \quad (36)$$

$$''R^{\bullet}_{r,2,w} + M_{1,w} \xrightarrow{k_{fm21}} ''P_r + R^{\bullet}_{1,w} \quad (37)$$

$$R^{\bullet}_{r,2,w} + M_{2,w} \xrightarrow{k_{fm22}} P_r + R^{\bullet}_{2,w} \quad (38)$$

$$''R^{\bullet}_{r,2,w} + M_{2,w} \xrightarrow{k_{fm22}} ''P_r + R^{\bullet}_{2,w} \quad (39)$$

Addition to terminal double bonds

$$''P_r + R^{\bullet}_{s,1,w} \xrightarrow{k_1^*} R^{\bullet}_{r+s,1,w} \quad (40)$$

$$''P_r + ''R^{\bullet}_{s,1,w} \xrightarrow{k_1^*} + ''R^{\bullet}_{r+s,1,w} \quad (41)$$

$$''P_r + R^{\bullet}_{s,2,w} \xrightarrow{k_2^*} + R^{\bullet}_{r+s,2,w} \quad (42)$$

$$''P_r + ''R^{\bullet}_{s,2,w} \xrightarrow{k_2^*} + ''R^{\bullet}_{r+s,2,w} \quad (43)$$

where, by analogy to the mechanism for unimolecular termination, reactions (41) and (43) are negligible compared with steps (40) and (42) since $[''R^{\bullet}] \ll [R^{\bullet}]$.

Termination by disproportionation

$$R^{\bullet}_{r,1,w} + R^{\bullet}_{s,1,w} \xrightarrow{k_{t11}} P_r + P_s \quad (44)$$

$$R^{\bullet}_{r,1,w} + ''R^{\bullet}_{s,1,w} \xrightarrow{k_{t11}} P_r + ''P_s \quad (45)$$

$$''R^{\bullet}_{r,1,w} + ''R^{\bullet}_{s,1,w} \xrightarrow{k_{t11}} ''P_r + ''P_s \quad (46)$$

$$R^{\bullet}_{r,1,w} + R^{\bullet}_{s,2,w} \xrightarrow{k_{t12}} P_r + P_s \quad (47)$$

$$R^{\bullet}_{r,1,w} + ''R^{\bullet}_{s,2,w} \xrightarrow{k_{t12}} P_r + ''P_s \quad (48)$$

$$''R^{\bullet}_{r,1,w} + R^{\bullet}_{s,2,w} \xrightarrow{k_{t12}} ''P_r + P_s \quad (49)$$

$$''R^{\bullet}_{r,1,w} + ''R^{\bullet}_{s,2,w} \xrightarrow{k_{t12}} ''P_r + ''P_s \quad (50)$$

$$R^{\bullet}_{r,2,w} + R^{\bullet}_{s,2,w} \xrightarrow{k_{t22}} P_r + P_s \quad (51)$$

$$R^{\bullet}_{r,2,w} + ''R^{\bullet}_{s,2,w} \xrightarrow{k_{t22}} P_r + ''P_s \quad (52)$$

$$''R^{\bullet}_{r,2,w} + ''R^{\bullet}_{s,2,w} \xrightarrow{k_{t22}} ''P_r + ''P_s \quad (53)$$

DERIVATION OF THE KINETIC MODEL

The derivation of the kinetic equations from the mechanism is analogous to the procedure outlined for homopolymers[56], and will only be highlighted in the following discussion.

Balance on macroradicals

$R^{\bullet}_r$ and $''R^{\bullet}_r$ are defined as macroradical chains with r monomer segment units. The superscript $''$ distinguishes

chains with terminal double bonds. The total macroradical concentration can be expressed as:

$$[R_T^\bullet] = [R^\bullet] + [''R^\bullet]$$

where

$$[R^\bullet] = \sum_{r=1}^{\infty} [R_r^\bullet] \quad \text{and} \quad [''R^\bullet] = \sum_{r=1}^{\infty} [''R_r^\bullet]$$

We may also distinguish between macroradicals with terminal monomer groups of type 1 ($R_1^\bullet$) and type 2 ($R_2^\bullet$). Therefore:

$$[R^\bullet] = [R_1^\bullet] + [R_2^\bullet]$$
$$[''R^\bullet] = [''R_1^\bullet] + [''R_2^\bullet]$$

We can also define:

$$[R_{1T}^\bullet] = [R_1^\bullet] + [''R_1^\bullet]$$
$$[R_{2T}^\bullet] = [R_2^\bullet] + [''R_2^\bullet]$$

where the subscript 'w' has been deleted from macroradical concentrations for brevity. For the remainder of the discussion it is, however, implied that all macromolecular species are expressed in aqueous-phase units.

The balance for macroradicals with terminal acrylamide units and no terminal double bonds* is:

$$\begin{aligned} d[R_1^\bullet]/dt = {} & k_{p1}[R_{in,w}^\bullet][M_{1,w}] + k_{p21}[R_2^\bullet][M_{1,w}] \\ & - k_{p12}[R_1^\bullet][M_{2,w}] - k_{fE}[R_1^\bullet]\Gamma_E \\ & + k_{fm21}[R_2^\bullet][M_{1,w}] - k_{fm12}[R_1^\bullet][M_{2,w}] \\ & - k_{t11}[R_1^\bullet][R_{1T}^\bullet] - k_{t12}[R_1^\bullet][R_{2T}^\bullet] \approx 0 \end{aligned} \quad (54)$$

The balance for macroradicals with terminal acrylamide units and a terminally unsaturated hydrocarbon is:

$$\begin{aligned} d[''R_1^\bullet]/dt = {} & k_{p1}[E^\bullet][M_{1,w}] + k_{p21}[''R_2^\bullet][M_{1,w}] \\ & - k_{p12}[''R_1^\bullet][M_{2,w}] - k_{fE}[''R_1^\bullet]\Gamma_E \\ & - k_{fm11}[''R_1^\bullet][M_{1,w}] - k_{fm12}[''R_1^\bullet][M_{2,w}] \\ & - k_{t11}[''R_1^\bullet][R_{1T}^\bullet] - k_{t12}[''R_1^\bullet][R_{2T}^\bullet] \approx 0 \end{aligned} \quad (55)$$

Summing equations (54) and (55) we obtain a balance for all types of macroradicals with terminal acrylamide groups. Analogous balances for macroradicals with terminal quaternary ammonium monomer units, with and without terminal double bonds, are:

$$\begin{aligned} d[R_2^\bullet]/dt = {} & k_{p2}[R_{in,w}^\bullet][M_{2,w}] + k_{p12}[R_1^\bullet][M_{2,w}] \\ & - k_{p21}[R_2^\bullet][M_{1,w}] - k_{fE2}[R_2^\bullet]\Gamma_E \\ & + k_{fm12}[R_1^\bullet][M_{2,w}] - k_{fm21}[R_2^\bullet][M_{1,w}] \\ & - k_{t22}[R_2^\bullet][R_{2T}^\bullet] - k_{t12}[R_2^\bullet][R_{1T}^\bullet] \approx 0 \end{aligned} \quad (56)$$

and

$$\begin{aligned} d[''R_2^\bullet]/dt = {} & k_{p2}[E^\bullet][M_{2,w}] + k_{p12}[''R_1^\bullet][M_{2,w}] \\ & - k_{p21}[''R_2^\bullet][M_{1,w}] - k_{fE2}[''R_2^\bullet]\Gamma_E \\ & - k_{fm21}[''R_2^\bullet][M_{1,w}] - k_{fm22}[''R_2^\bullet][M_{2,w}] \\ & - k_{t22}[''R_2^\bullet][R_{2T}^\bullet] - k_{t12}[''R_2^\bullet][R_{1T}^\bullet] \approx 0 \end{aligned} \quad (57)$$

By summing equations (56) and (57) the total balance for macroradicals with terminal cationic monomer groups can be derived. Alternatively, we can calculate the overall macroradical concentration by summing equations (54)–(57)†:

$$\begin{aligned} d[R^\bullet]/dt = {} & R_I + R_I' - \Gamma_E(k_{fE}[R_{1T}^\bullet] + k_{fE2}[R_{2T}^\bullet] \\ & - k_{t11}[R_{1r}^\bullet]^2 + 2k_{t12}[R_{1T}^\bullet][R_{2T}^\bullet] \\ & - k_{f22}[R_{2T}^\bullet]^2 \approx 0 \end{aligned} \quad (58)$$

where R_I and R_I' are the rates of initiation from primary and emulsifier radicals. These can respectively be expressed as:

$$R_I = [R_{in,w}^\bullet](k_{p1}[M_{1,w}] + k_{p2}[M_{2,w}])$$
$$R_I' = [E^\bullet](k_{p1}[M_{1,w}] + k_{p2}[M_{2,w}])$$

Invoking the long-chain approximation, the concentration of macroradicals with terminal acrylamide and quaternary ammonium groups can be related:

$$\begin{aligned} k_{p21}[M_{1,w}][R_{2T}^\bullet] &= k_{p12}[M_{2,w}][R_{1T}^\bullet] \pm 1 \\ &\approx k_{p12}[M_{2,w}][R_{1T}^\bullet] \end{aligned}$$

Therefore

$$[R_{2T}^\bullet] = \frac{k_{p12}}{k_{p21}} \frac{[M_{2,w}]}{[M_{1,w}]} [R_{1T}^\bullet] \quad (59)$$

and

$$[R_T^\bullet] = [R_{1T}^\bullet]\left(1 + \frac{k_{p12}}{k_{p21}} \frac{[M_{2,w}]}{[M_{1,w}]}\right) \quad (60)$$

Substituting equation (59) into (58) and simplifying:

$$R_I + R_I' - k_{fE,group}[R_{1T}^\bullet]\Gamma_E - k_{td,group}[R_{1T}^\bullet]^2 \approx 0 \quad (61)$$

where $k_{fe,group}$ and $k_{td,group}$ are grouped pseudo-rate constants for transfer to emulsifier and disproportionation termination. These are expressed as:

$$k_{fE,group} = k_{fE} + k_{fE2}\left(\frac{k_{p12}}{k_{p21}} \frac{[M_{2,w}]}{[M_{1,w}]}\right) \quad (62a)$$

$$\begin{aligned} k_{td,group} = {} & k_{t11} + 2k_{t12}\left(\frac{k_{p12}}{k_{p21}} \frac{[M_{2,w}]}{[M_{1,w}]}\right) \\ & + k_{t22}\left(\frac{k_{p12}}{k_{p21}} \frac{[M_{2,w}]}{[M_{1,w}]}\right)^2 \end{aligned} \quad (62b)$$

where

$$k_{t12} = 2(k_{t11}k_{t22})^{1/2} \quad (62c)$$

The balance on emulsifier radicals is given by:

$$\begin{aligned} d[E^\bullet]/dt = {} & k_{fE,group}[R_{1T}^\bullet]\Gamma_E - k_{p1}[E^\bullet][M_{1,w}] \\ & - k_{p2}[E^\bullet][M_{2,w}] - k_5[E^\bullet][HC_{imp}] \approx 0 \end{aligned} \quad (63)$$

Rearranging equation (63) in terms of R_I':

$$R_I' = \frac{k_{fE,group}[R_{1T}^\bullet]\Gamma_E}{1 + k_5[HC_{imp}]/(k_{p11}[M_{1,w}] + k_{p22}[M_{2,w}])} \quad (64)$$

Combining equations (61) and (63) yields:

$$2fk_d[I] - k_{fE,group}(1 - f_e)[R_{1T}^\bullet]\Gamma_E - k_{td,group}[R_{1T}^\bullet]^2 \approx 0 \quad (65)$$

* It will be assumed that primary radicals are the dominant transferring species between phases. The partitioning of macroradicals with length greater than 1 is therefore, as a first approximation, completely in the aqueous phase

† Transfer to monomer from macroradicals containing unsaturated hydrocarbons has been neglected since $k_{fm}[''R^\bullet] \ll k_p[R_{in}^\bullet]$

where

$$f_e = \frac{1}{1 + k_5[HC_{imp}]/(k_{p11}[M_{1,w}] + k_{p22}[M_{2,w}])}$$

This is analogous to the expression for the efficiency of initiation by emulsifier radicals derived for homopolymers[56].

Equation (65) is a quadratic, which can be solved for $[R^{\bullet}_{1T}]$. The concentrations $[R^{\bullet}_{2T}]$ and $[R^{\bullet}_{T}]$ can then be computed from equations (59) and (60) respectively.

Monomer consumption rate

The rate of consumption of acrylamide and the quaternary ammonium monomer can be expressed as:

$$-d[M_{1,w}]/dt = k_{p11}[M_{1,w}][R^{\bullet}_{1T}] + k_{p21}[M_{1,w}][R^{\bullet}_{2T}]$$

$$-d[M_{2,w}]/dt = k_{p22}[M_{2,w}][R^{\bullet}_{2T}] + k_{p12}[M_{2,w}][R^{\bullet}_{1T}]$$

or in a more convenient form:

$$d[M_{1,w}]/dt = -k_{p11}[R^{\bullet}_{1T}]([M_{1,w}] + [M_{2,w}]/r_1) \quad (66)$$

$$d[M_{2,w}]/dt = -k_{p12}[R^{\bullet}_{1T}]([M_{2,w}] + r_2[M_{2,w}]^2/[M_{1,w}]) \quad (67)$$

From equations (66) and (67) it is clear that the relative consumption rate of the monomers ($d[M_1]/d[M_2]$) and the copolymer composition are determined exclusively from the reactivity ratios and the monomer concentrations, and are independent of all other experimental conditions. This will later be tested experimentally.

Balance on initiator

$$d[I]/dt = -k_d[I] \quad (68)$$

The efficiency of initiation of primary radicals

By an identical procedure to that described for homopolymers[56], the efficiency of initiation can be shown to be expressed by:

$$f = \left[1 + \frac{\Phi_r}{k_r^*}\left(\frac{k_1[HC]}{a_{sp}} + \frac{k_4[E_0]}{a_{sp}} + \frac{k_{p1}[M_{1,w}]\Phi_{m1}}{a_{sp}} + \frac{k_{p2}[M_{2,w}]\Phi_{m2}}{a_{sp}}\right)\right]^{-1} \frac{V_o}{V_w}$$

For the special case where the efficiency does not depend on monomer concentration, this can be simplified to yield:

$$f = \left[1 + \frac{\Phi_r}{k_r^*}\left(\frac{k_1[HC]}{a_{sp}} + \frac{k_4[E_0]}{a_{sp}}\right)\right]^{-1} \frac{V_o}{V_w} \quad (69)$$

where k_r is the mass transfer constant for primary radicals, defined as:

$$k_r = k_r^* a_{sp} V_o$$

a_{sp} is the specific interfacial area per litre of oil:

$$a_{sp} = a_T/V_o$$

a_T is the total interfacial area (m^2) and V_o the volume of the oil phase.

Equations for conversion and composition

The molar (X) and mass (X_m) conversions are respectively given by:

$$X = 1 - \frac{[M_{1,w}] + [M_{2,w}]}{[M_{1,w}]^0 + [M_{2,w}]^0} \quad (70)$$

$$X_m = 1 - \frac{Mw_1[M_{1,w}] + Mw_2[M_{2,w}]}{Mw_1[M_{1,w}]^0 + Mw_2[M_{2,w}]^0} \quad (71)$$

where Mw_1 and Mw_2 are the molar masses of acrylamide and the quaternary ammonium cationic monomer. The superscript "0" denotes an initial concentration.

The monomer and cumulative polymer compositions are given by:

$$f_1 = [M_{1,w}]/([M_{1,w}] + [M_{2,w}]) \quad (72)$$

$$\bar{F}_1 = 1 - \frac{[M_{1,w}]^0 - [M_{1,w}]}{[M_{1,w}]^0 + [M_{2,w}]^0 - [M_{1,w}] - [M_{2,w}]} \quad (73)$$

Therefore equations (62) and (65)–(73) constitute the kinetic model for inverse-microsuspension copolymerization.The coupled differential equations will be solved by a sixth-order Runge–Kutta procedure.

EXPERIMENTAL PLAN

The generalization of the inverse-microsuspension mechanism to copolymers and electrolytes requires several physical and kinetic parameters. These include propagation, termination and cross-termination constants for the cationic monomers, reactivity ratios for quaternary ammonium monomers with acrylamide, mass-transfer and partition coefficients for monomers and radicals, and an estimate of the magnitude of diffusion-controlled termination. With the exception of the reactivity ratios, these parameters have not been determined. The following three-phase experimental programme is proposed such that independent parameter estimates can be elucidated from kinetic, latex characterization and partitioning measurements.

A preliminary set of homopolymerizations of DMAEA and DMAEM will be conducted to determine the Arrhenius dependence of the rate parameter $k_p/k_t^{1/2}$. Experiments will be performed isothermally between 40 and 60°C in solution and inverse microsuspension, and combined with available literature data for other temperatures.

A second set of experiments will spectrometrically measure the partitioning of acrylamide, DMAEA and DMAEM between water and Isopar-K, the dispersion medium used for inverse-microsuspension polymerizations. These partition coefficients will enable the kinetic model to distinguish macromolecular chain addition in the aqueous phase from oligoradical propagation in the organic medium. Experiments will be performed over a range of phase ratios and emulsifier concentrations (sorbitan monooleate) in order to mimic the conditions that exist in inverse-microsuspension polymerization.

The final stage of this research, and the principal objective of this paper, involves the inverse-microsuspension copolymerization of acrylamide with quaternary ammonium cationic monomers. Experiments will be performed with DMAEA and DMAEM at 50 wt% monomer concentration. An oil-soluble azo initiator, azobisisobutyronitrile (AIBN), will be employed with reactions performed isothermally over the temperature range 40–60°C. These conditions correspond approxi-

mately to commercial polymerization recipes. Based on measurements of the residual monomer concentrations, the kinetic model will be compared with experimental rate and copolymer composition data. This will be used to evaluate the suitability of the reactivity ratios, estimated in aqueous solution polymerization, for heterophase processes. Further, it will allow the elucidation of three new physical and kinetic parameters: the mass-transfer coefficient of oligoradicals between the aqueous and organic phases; the magnitude of the diffusional limitations on termination; and the decoupling of the propagation and termination rate parameters.

EXPERIMENTAL

Reagent purification

Dimethylaminoethyl acrylate (DMAEA) and dimethylaminoethyl methacrylate (DMAEM) were obtained as concentrated (75 wt%) aqueous solutions, inhibited with 1000 ppm of hydroquinone monomethyl ether (MeHQ) (CPS Chemical Co.). The DMAEM was further stabilized with 10 ppm of cupric ions, as determined by optical emission spectroscopy (Jarrett Ash Division ICAP 9000) using copper nitrate to calibrate the instrument. The quaternary ammonium monomers were purified to MeHQ levels of <0.5 ppm by repetitive extractions with acetone (BDH, reagent grade). In this novel procedure, the raffinate is purified by extracting MeHQ, Cu^{2+} and water in the supernatant (acetone). With each stage, the concentration of the quaternary ammonium in the raffinate increases until a sufficient portion of the moisture was removed to allow the monomer to crystallize. The solids were subsequently filtered and washed with acetone.

Solid acrylamide monomer (Cyanamid BV, The Netherlands) was recrystallized from chloroform (Caledon, reagent grade) and washed with benzene (BDH, reagent grade).

The initiators azobisisobutyronitrile (Kodak) and potassium persulphate (Fisher, 'certified' minimum assay 99.5%) were recrystallized from methanol (BDH, reagent grade) and doubly distilled deionized water respectively.

All reagents were dried *in vacuo* to constant weight and stored separately in desiccators over silica gel.

Determination of monomer and polymer composition

Copolymer compositions were inferred from chromatographic measurements of the residual monomer concentration. A high-performance liquid chromatography method, developed for the simultaneous detection of acrylamide and quaternary ammonium cationic monomers[47], was employed. This has a sensitivity of below 1 ppm, with a reproducibility (95% confidence intervals) of $\pm 0.25\%$.

The h.p.l.c. stationary phase consisted of a CN column (9% groups bonded to a μ-Porasil (silica) substrate, Waters Assoc.) with an 8 mm i.d. and 4 μm particles. The column was housed in a radial compression system (RCM-100, Waters) and was operated at a nominal pressure of 180 kg cm^{-2}. The h.p.l.c. system consisted of a degasser (ERC-3110, Erma Optical Works), a Waters U6K injector, a stainless-steel filter and a CN precolumn (Waters). An ultra-violet detector (Beckman 160) with a zinc lamp operating at a wavelength of 214 nm was used to measure the monomer absorption. A Spectra-Physics SP4200 integrator was used to compute peak areas. The mobile phase was a mixture of 50 vol% acetonitrile (Caledon, distilled in glass, u.v. grade) and 50 vol% doubly distilled deionized water, containing 0.005 mol l^{-1} dibutylamine phosphate. The flow rate was 2.0 ml min^{-1}. The quaternary ammoniums were retained longer in the column due to adsorption onto the polar groups of the packing. This peak separation was optimized by varying the acetonitrile/water ratio.

Residual monomer concentrations were determined on polymer samples treated as follows: A 2 ml portion of the reactor sample was centrifuged for 16 h in an Adams Analytical Centrifuge to separate the organic and aqueous phases. The supernatant layer phase was syringed off and a sample of the remaining polymer–monomer–water mixture (nominally 0.01 g) was removed, weighed to five decimal places, and immersed in 20.00 ml of doubly distilled deionized water. This was subsequently sealed in a 20 ml vial and agitated vigorously with a magnetic stirrer until dissolved. Homogenized samples were filtered through a 0.45 μm cellulose acetate nitrate filter (Millipore) and diluted, if necessary, to obtain a monomer concentration below 100 ppm. Then 100 μl of each sample was injected into the h.p.l.c. using a 100 μl glass syringe (Scientific Glass Engineering Ltd). Four replications were performed. Residual monomer concentrations were determined from a regressed calibration curve derived from standard samples from 0* to 100 ppm, prepared with recrystallized and vacuum-dried monomer. The absorption–concentration dependence followed Beer's law up to 100 ppm for acrylamide and 500 ppm for the cationic monomers.

Polymerization procedure

Purified monomers were removed from their storage desiccators and dissolved at the appropriate concentration in distilled deionized water. Mild heating was required to overcome the negative enthalpy of dilution†. A thermometer was immersed in the solution and the temperature was maintained below 20°C during this procedure. When dissolved, the monomer solution was covered and purged with rarefied nitrogen (UHP grade, 99.999% purity, Canadian Liquid Air) for 15–30 min. Purging was stopped when the residual oxygen level dropped below 1.5 ppm, as measured with a dissolved oxygen probe (Yellow Springs Instrument Co., model 54). A presample of this solution was taken to measure the initial monomer composition. The organic phase was prepared by weighing the appropriate amounts of Isopar-K‡ (Esso Chemicals) and sorbitan monooleate (Alkaril Chemicals Ltd). The emulsifier dissolved readily in the isoparaffinic solvent and the mixture was purged with nitrogen for 10–20 min. The initiator solution was prepared by dissolving recrystallized AIBN in 15 g of acetone.

The reactor loading procedure was as follows: to a well cleaned one-gallon stainless-steel batch reactor (Chemineer), the degassed organic phase was charged. The aqueous phase was subsequently added and the

* At 0 ppm, a negative peak due to the solvent (water) front was observed

† The dilution of acrylamide in water is endothermic (-2.9 kcal mol^{-1}) owing to the formation of hydrogen-bonded molecular dimers in the solid state[63], which require excess energy to dissociate

‡ This reagent was used as received

system pre-emulsified. The reactor was then sealed and agitation (323 ± 1 r.p.m.) was commenced. Nitrogen sparging at a very slow rate (< 20 ml s^{-1}) was continued for the duration of the polymerization. The temperature was ramped slowly (3°C min^{-1}) until the set point was reached. After thermal instabilities were reduced to below ± 1°C for a period of no less than 5 min, a presample was taken and the initiator solution was added. A 20 ml glass syringe (Multifit) was used to inject the initiator solution through a resealable hole in the top of the reactor. The agitation was stopped for approximately 20 s during the initiator addition. The mid-time of the addition was noted and taken as the commencement of the polymerization. A PID controller varied the steam/chilled water feed ratio entering the cooling jacket. Temperature control was excellent for all polymerizations, with deviations always below 1°C, including an initial perturbation when the initiator was added.

Samples were withdrawn periodically at time intervals of at least 5 min in order to obtain 20 well spaced conversion–time data for each experiment. The sampling procedure was as follows: A sampling valve at the bottom of the reactor was opened and approximately 5 ml of sample was drained to waste. A 20 ml glass sample bottle containing 0.1 ml of a 1 wt% hydroquinone (Aldrich) solution was placed below the valve and filled. This provided an aqueous-phase concentration of hydroquinone of 100 ppm, sufficient to scavenge any unreacted radicals and stop the polymerization. The sample was vigorously shaken and immersed in an ice bath. The exact time (hours:minutes:seconds) of sample withdrawal was then recorded. At the conclusion of the experiment the samples were refrigerated at 10°C prior to centrifugation.

For homopolymerizations in inverse microsuspension the same procedure was employed. In solution polymerizations the aqueous-phase treatment was identical. However, the reaction was initiated with a water-soluble initiator (recrystallized potassium persulphate, $K_2S_2O_8$). For solution polymerizations, the preparation of samples for h.p.l.c. consisted exclusively of dilution and filtration.

Polymerization conditions

Inverse-microsuspension copolymerizations of acrylamide (AAM) with dimethylaminoethyl acrylate (DMAEA) or dimethylaminoethyl methacrylate (DMAEM) were performed isothermally over the temperature range 40–60°C. A low dispersed phase ratio (0.74:1) was used to reduce the heat generation rate and improve the thermal stability. The cationic monomer fraction was kept low (25 wt%) to duplicate commercial recipes. An oil-soluble azo initiator (AIBN) was used with Isopar-K, a narrow-cut isoparaffinic mixture, as a dispersion medium. Sorbitan monooleate, common to several industrial heterophase polymerizations of water-soluble monomers (Srinivason[64] (Nalco), Easterly[65] (Dow), Becher[66] (Allied)), was employed as the stabilizer. The specific reaction conditions for each experiment are listed in *Table 3*.

Monomer partitioning measurements

Ultra-violet spectrometry was used to measure the partitioning of AAM, DMAEA and DMAEM between aqueous monomer solutions and hydrocarbons. Experiments were performed at monomer concentrations of 0.5 and 1.4 mol l^{-1}, prepared with doubly distilled deionized water. Isopar-K and sorbitan monooleate constituted the oil phase. For each monomer a series of samples with organic to aqueous phase ratios of 1:1, 2:1 and 4:1 were prepared with oil phases containing 1, 4 and 8 wt% emulsifier. Samples were agitated vigorously for a period of approximately 6 h to ensure that equilibrium partitioning was obtained. The phases were then separated by a two-stage centrifugation procedure. The Isopar-K was separated from the aqueous phase by centrifuging for 10 min in a Sorvall RC5B Superspeed Centrifuge operated at 11 000*g*. This was subsequently centrifuged in an Eppendorf model 5415 Centrifuge operated at 14 000*g* to separate the emulsifier. This was continued until the aqueous phase was clear.

The partition coefficient was calculated by measuring the initial and equilibrium monomer concentration in the aqueous phase. An ultra-violet spectrophotometer with variable-wavelength detector (Gilford Response) was used. The measurement wavelengths were: 200 nm for DMAEA, 212 nm for AAM and 220 nm for DMAEM. These corresponded to the maximum u.v. absorption for each monomer. The absorbance was translated to a mass concentration by calibrating with standards between 1 and 100 ppm.

Particle-size measurement

Particle sizes were determined by dynamic light scattering (Nicomp 370, Pacific Scientific) and optical

Table 3 Experimental conditions for polymerizations with cationic monomers

Temperature (°C)	Initiator	Cationic monomer	Initiator concentration $(10^{-3}$ mol $l^{-1})_o$	Total monomer concentration (mol $l^{-1})_w$	f_{1o}[a]	Mass of emulsifier (SMO, g)	Mass of aqueous phase (g)	Mass of oil (Isopar-K) (g)	$\Phi_{w/o}$
60	AIBN	DMAEM	3.327	0.637	0.0	100.1	1000.1	1000.1	0.74
60	$K_2S_2O_8$	DMAEA	0.127[b]	0.350	0.0	0.0	2000.0	0.0	–
60	AIBN	DMAEM	3.329	6.09	0.875	100.0	1000.0	1000.7	0.74
50	AIBN	DMAEM	7.373	6.11	0.875	100.0	1000.1	1000.0	0.74
40	AIBN	DMAEM	14.83	6.13	0.877	100.0	1004.0	1000.0	0.74
60	AIBN	DMAEA	3.337	6.05	0.840	100.0	1018.2	1018.2	0.74
40	AIBN	DMAEA	14.81	6.13	0.853	100.0	1000.1	1000.0	0.74

[a] For copolymerizations with acrylamide
[b] Potassium persulphate (mol $l^{-1})_w$

photomicrography. In the former a helium–neon laser operating at 633 nm was used to measure the mean diffusion coefficient of the particles. Diameters are then inferred using the Stokes–Einstein relationship. Measurements were performed at 23°C with disposable glass stationary cells. Autocorrelation functions were accumulated for periods ranging from 25 min to 3.5 h. All samples were measured at least twice. Solutions with a nominal concentration of 1 wt% were prepared by diluting inverse-microsuspension samples with Isopar-K. This concentration has been found to be ideal for the characterization of inverse latices[67]. Photomicrographs were taken with Kodak TMAX-3200 and Tri X-400 black and white film at 250 × magnification. A Lietz Labor/UX microscope equipped with NPL objectives was used. Particle-size distributions were determined from photomicrographs by measuring at least 400 images. *Figure 1* shows sample photographs taken under normal, uneven and dark-field illumination.

RESULTS AND DISCUSSION

Homopolymerization of cationic monomers

Figure 2 shows the experimental conversion–time data for the inverse-microsuspension polymerization of DMAEM at 60°C. The monomer and initiator concentrations were 0.637 mol l^{-1} and 3.327×10^{-3} mol l^{-1} respectively. Under such conditions, primary radical generation is principally due to the thermal bond rupture of the azo group, which results in a predominance of bimolecular macroradical termination. The inverse-microsuspension kinetic model therefore reduces to the classical free-radical rate expression:

$$R_p = (2fk_d[I])^{1/2}(k_p/k_t^{1/2})[M]$$

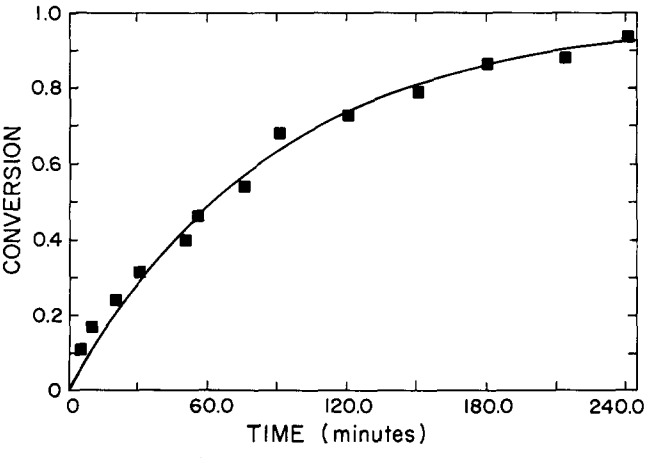

Figure 2 Kinetics of the inverse-microsuspension homopolymerization of DMAEM at 60°C: (■) conversion data measured by h.p.l.c.; (———) model prediction. Experimental conditions: [monomer] = 0.637 mol l_w^{-1}, [AIBN] = 3.327×10^{-3} mol l_o^{-1}, $\phi_{w/o} = 0.74$

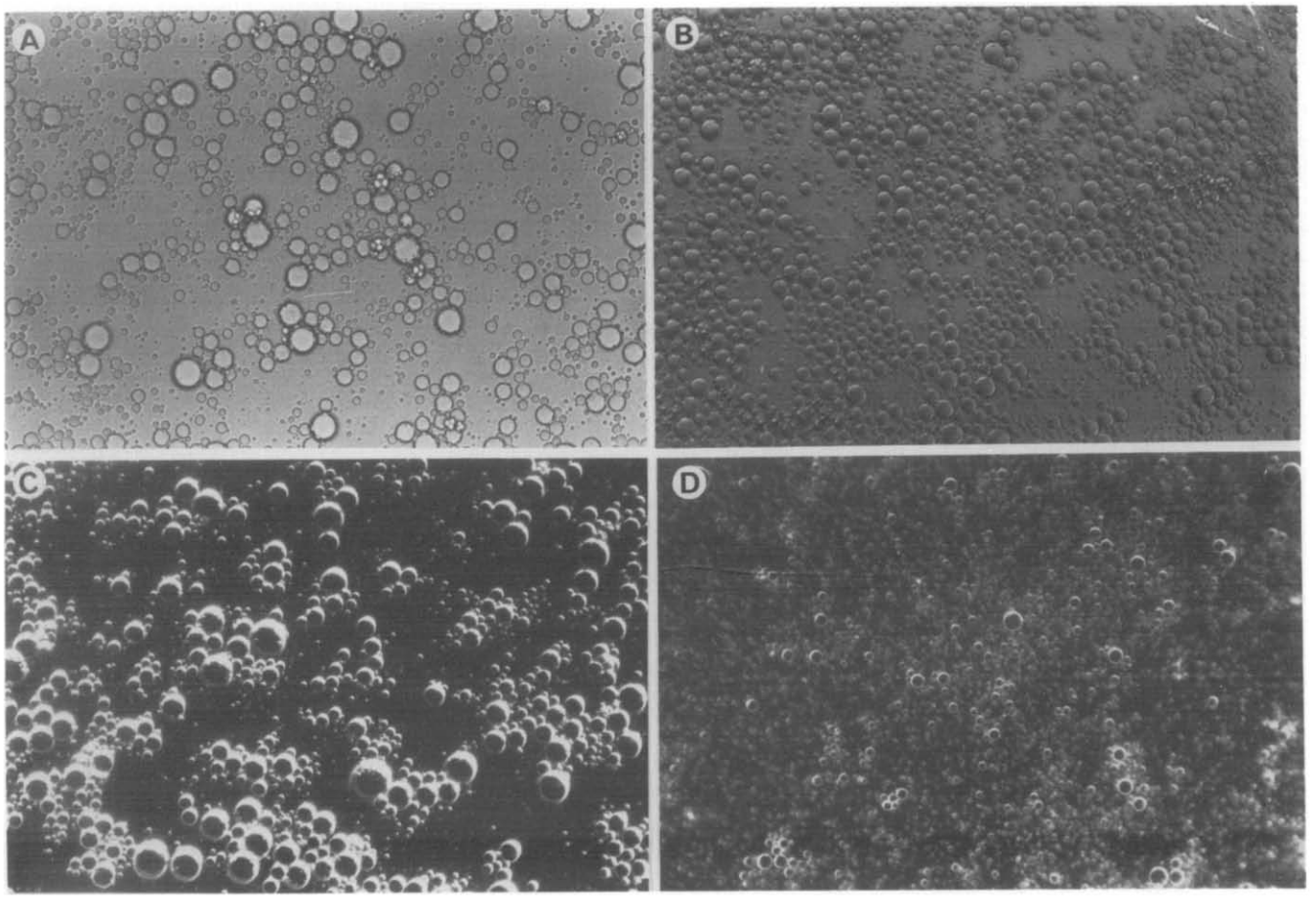

Figure 1 Optical photomicrographs. (A) Photomicrograph of an AAM/DMAEA copolymer produced at 60°C under the following experimental conditions: [monomer] = 6.05 mol l_w^{-1}, [AIBN] = 3.337×10^{-3} mol l_o^{-1}, $f_{10} = 0.840$, $\phi_{w/o} = 0.74$. (B) Photomicrograph taken with uneven illumination to provide relief to the particle images. (C) Photomicrograph taken with a dark-field substage condenser, providing the appearance of a three-dimensional image. (D) Photomicrograph taken with a dark-field substage condenser. The white particle outlines allow for unambiguous particle diameter measurements.

Table 4 Experimental values of activation energy of DMAEM polymerization in the literature

E_a (kcal mol^{-1})	Reference
17.0[a]	Egoyan[35]
17.85	Luskin[68]
19.20	Gerduilite[69]
19.88	Katime[70]

[a]Invariant to solvent composition

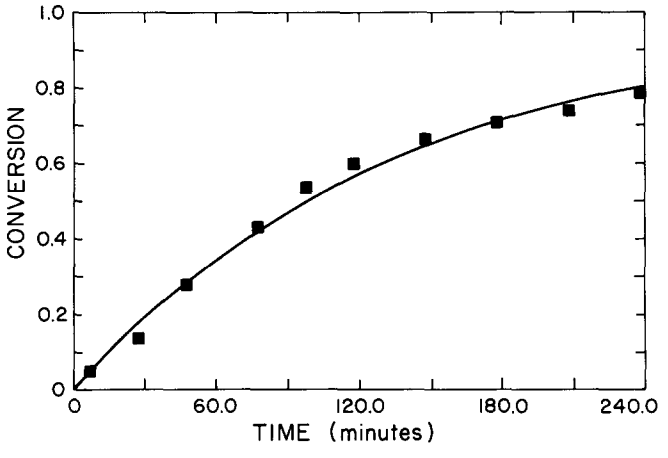

Figure 3 Kinetics of the aqueous solution polymerization of DMAEA at 60°C: (■) conversion data measured by h.p.l.c.; (———) model prediction. Experimental conditions: [monomer] = 0.350 mol l$_w^{-1}$, [$K_2S_2O_8$] = 0.127 × 10^{-3} mol l$_w^{-1}$

with the heterophase initiation efficiency defined as:

$$f = \left[1 + \frac{\Phi_r}{k_r^*}\left(\frac{k_4[HC]}{a_{sp}} + \frac{k_1[E_0]}{a_{sp}}\right)\right]^{-1} \frac{V_o}{V_w}$$

For the reaction conditions listed above, with a concentration of sorbitan monooleate of 0.388 mol l^{-1}, and a measured average particle diameter of 7 μm, the calculated heterophase efficiency is 0.03. Using this value the kinetic parameter $k_p/k_t^{1/2}$ and its 95% confidence intervals have been estimated from the conversion data:

$$(k_p/k_t^{1/2})_{DMAEM,60°C} = 32.73 \pm 2.17\ l^{1/2}\ mol^{-1/2}\ min^{-1/2}$$

Previous experimental values for the activation energy of DMAEM polymerizations are summarized in *Table 4*. Although these magnitudes are quite large, E_a is typically of the order 5 kcal mol^{-1}, they appear reliable in light of the very low rates found in this research for polymerizations at 40°C ($R_p \approx 0$ over 5 h). Using the median activation energy from *Table 4*, the following Arrhenius expression for $k_p/k_t^{1/2}$ is obtained:

$$(k_p/k_t^{1/2})_{DMAEM} = 1.68 \times 10^{13} \exp(-17850/RT)\ l^{1/2}\ mol^{-1/2}\ min^{-1/2}$$

Figure 3 shows the conversion–time data for the potassium-persulphate-initiated polymerization of DMAEA in aqueous solution. The corresponding monomer and initiator levels were 0.350 mol l^{-1} and 1.27 × 10^{-4} mol l^{-1} respectively. The classical free-radical polymerization expression can again be applied to these kinetics provided an estimate of the initiator decomposition rate ($k_d = 2.12 \times 10^{18} \exp(-33320/RT)$[71,72] and the efficiency of initiation are available. For reactions with highly purified reagents in contaminant-free media,

Table 5 Monomer partitioning between aqueous and organic phases[a]

Composition of the organic phase (wt% sorbitan monooleate)	$n_{o/w}$[b]		
	Acrylamide	DMAEA	DMAEM
1.0	0.0153	0.0107	0.0113
4.0	0.0170	0.0121	0.0279
8.0	0.0201	0.0208	0.0347

[a]The aqueous phase consisted of 1.4 mol l^{-1} of monomer in doubly distilled deionized water. Isopar-K and sorbitan monooleate comprised the organic phase
[b](mol l^{-1})$_o$/(mol l^{-1})$_w$

Riggs[73], Singh[74] and Kim[75] have indicated that f deviates insignificantly from unity. Using an arbitrary value of $f = 1.0$ the rate parameter $k_p/k_t^{1/2}$ can be estimated:

$$(k_p/k_t^{1/2})_{DMAEM,60°C} = 25.29 \pm 1.99\ l^{1/2}\ mol^{-1/2}\ min^{-1/2}$$

The 95% confidence limits are narrow, as was also found for DMAEM. This reflects the accuracy of the h.p.l.c. method for residual monomer concentration determination. Furthermore, the magnitude was near* to what was estimated for DMAEM, as was expected based on prior research. This is significant since $k_p/k_t^{1/2}$ was determined for DMAEM in inverse microsuspension and for DMAEA in solution. This suggests that the calculated value for the heterophase initiator efficiency, and indeed the entire heterophase initiation efficiency model developed herein and in a prior publication[56], are reliable and consistent with independent experimental observation.

Using Luskin's value of the activation energy for DMAEA polymerizations, the Arrhenius expression for $k_p/k_t^{1/2}$ is:

$$(k_p/k_t^{1/2})_{DMAEA} = 7.61 \times 10^{13} \exp(-19020/RT)\ l^{1/2}\ mol^{-1/2}\ min^{-1/2}$$

Monomer partitioning between aqueous and organic phases

The partition coefficient of acrylamide between doubly distilled deionized water and Isopar-K, with 1 wt% sorbitan monooleate, was experimentally determined to be 0.0153. This is in excellent agreement with Glukhikh's[76] result ($n = 0.02$) measured with toluene as an organic phase. Furthermore, since the partitioning of the quaternary ammonium monomers was also found to be significantly greater than zero (*Table 5*), the mechanism for initiation in inverse microsuspension, developed herein, can therefore be generalized to include copolymerizations of acrylamide with these cationic monomers. This will be discussed in the following section of the paper.

The partitioning measurements also demonstrate that sorbitan emulsifiers promote the solubility of acrylamide and dimethylamines in aliphatic media. This was originally postulated by McKechnie[77] and provides experimental verification of Candau's[78] inference that the interfacial region in inverse-microemulsion polymeriza-

* With the efficiency of initiation arbitrarily set at 0.77, a very plausible value for potassium persulphate, $k_p/k_t^{1/2}$ is identical for DMAEA and DMAEM

Table 6 Summary of kinetic constants for the copolymerization of acrylamide and quaternary ammonium monomers

Parameter	Value	Units
(1) AAM/DMAEM		
r_1	$7.823\exp(-923/T)$	Dimensionless
r_2	$4.538\exp(-204/T)$	Dimensionless
$(k_p/k_t^{1/2})_{DMAEM}$	$1.68\times10^{13}\exp(-17850/RT)$	$l^{1/2}\,mol^{-1/2}\,min^{-1/2}$
$(k_p/k_t)_{DMAEM}$	$\approx1.31\times10^{9}\exp(-17850/RT)^a$	Dimensionless
A	0.0	Dimensionless
$k_1\Phi_r/k_r^*$	2.24×10^{3}	$m^2\,mol^{-1}$
$k_4\Phi_r/k_r^*$	5.66×10^{1}	$m^2\,mol^{-1}$
k_1/k_4	39.5	Dimensionless
(2) AAM/DMAEA		
r_1	$1.871\times10^{-2}\exp(913/T)$	Dimensionless
r_2	$1.083\times10^{-2}\exp(1148/T)$	Dimensionless
$(k_p/k_t^{1/2})_{DMAEA}$	$7.61\times10^{13}\exp(-19020/RT)$	$l^{1/2}\,mol^{-1/2}\,min^{-1/2}$
$(k_p/k_t)_{DMAEA}$	$\approx5.093\times10^{9}\exp(-19020/RT)^a$	Dimensionless
A	0.0	Dimensionless
$k_1\Phi_r/k_r^*$	7.785×10^{3}	$m^2\,mol^{-1}$
$k_4\Phi_r/k_r^*$	1.970×10^{2}	$m^2\,mol^{-1}$
k_1/k_4	39.5	Dimensionless

$^a E_T = E_p - E_t \approx E_p$ given the large magnitude of E_p and the general tendency for low activation energies for macroradical termination reactions

tion contains appreciable levels of unreacted monomer. The monomer–emulsifier interaction also provides a credible explanation for the interfacial propagation reaction proposed by Hunkeler[56] and used for the mechanism (steps (29) and (30)) in this paper.

Inverse microsuspension: parameter estimation

From the kinetic model there are five unknown parameters: k_{p22}, k_{t22}, k_{fe22}, k_r^* and A, the gel effect parameter defined in:

$$k_{td} = k_{td}^{\circ}/\exp(Aw_p)$$

where w_p is the weight fraction of polymer in the aqueous phase. Of these parameters only four are independent, since the propagation and termination kinetic constants are coupled through the ratio $k_{p22}/k_{t22}^{1/2}$. Furthermore, unimolecular termination with emulsifier is probably controlled by the diffusion of the macroradical to the interface. In this case the chemical composition of the reactive end-group is inconsequential, and transfer to emulsifier occurs at approximately equal rates for macroradicals with terminal acrylamide and cationic groups. It is therefore a valid approximation to write $k_{fe2} \approx k_{fe}$.

The remaining three parameters can be estimated independently from the rate and particle-size data. The propagation rate constant (k_{p22}) will influence the initial rate of polymerization, the gel effect parameter (A) will be of primary consequence at high conversions and the mass-transfer constant (k_r^*) will be inferred from measurements of the total interfacial area of the latex.

These will be estimated from the conversion and average particle diameter data using a weighted non-linear least-squares algorithm based on Marquardt's procedure. All experiments for a given monomer pair will be fitted in a single estimation routine so that the activation energies of these parameters can be estimated directly. This is preferable to estimating unique parameters for each experiment, since the latter procedure is susceptible to over-fitting inaccurate data, and therefore is incapable of isolating inconsistent results.

The results of the parameter estimation are given in *Table 6*. The efficiency of initiation for DMAEM copolymerizations was 0.52 compared with 0.21 for DMAEA. This is consistent with the monomer partitioning experiments, which determined that the solubility of DMAEM in the continuous phase is 67% larger than that of DMAEA, at high emulsifier levels (*Table 5*). Propagation in the continuous phase will therefore be favoured for DMAEM relative to DMAEA, which will reduce the fraction of radicals scavenged by hydrocarbon-phase impurities and increase the efficiency of initiation. This is strong evidence that the proposed oligoradical nucleation mechanism (steps (13) and (14)) is correct.

For these copolymers the efficiency of initiation was found to be invariant with temperature, as was also observed for acrylamide homopolymers[56].

The quoted propagation constants for the cationic monomers are approximate, and rigorously should be determined by a non-stationary method such as the rotating sector, or by direct measurement of the radical concentration by electron spin resonance. The magnitudes of the propagation rates are: $k_{p22,DMAEM} > k_{p22,DMAEA} \gg k_{p22,AAM}$. This seems reasonable given the greater tendency for quaternary ammonium monomers to polymerize spontaneously.

For copolymerizations with either dimethylamine, the gel effect parameter was not significantly greater than zero ($A < 10^{-4}$) and was therefore eliminated.

The absence of diffusional limitations on bimolecular termination is probably the result of two effects: lower molecular weights in cationic copolymerizations relative to acrylamide homopolymers, and electrostatic interactions. Both of these reduce the density of chain entanglements and the gel effect*. The latter phenomenon

* In acrylamide homo- and copolymerizations, the predominant diffusion limitation is the result of chain entanglements between the high-molecular-weight macromolecules. Free-volume influences are negligible owing to the high fraction of solvent in the reaction mixture

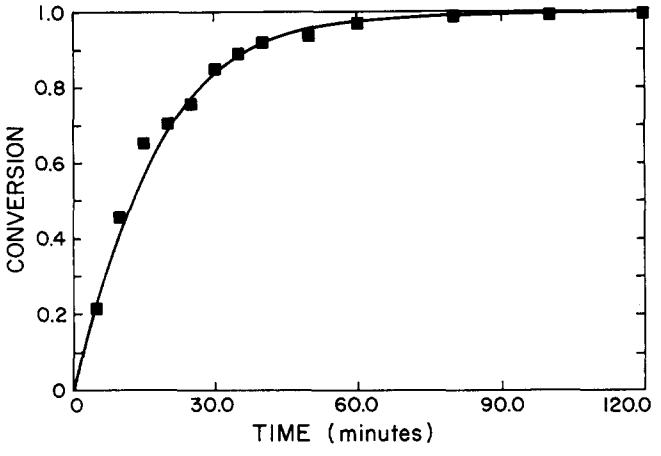

Figure 4 Conversion–time data (■) and kinetic model predictions (———) for an AAM/DMAEM copolymerization at 60°C. Experimental conditions: [monomer] = 6.09 mol l_w^{-1}, [AIBN] = 3.329×10^{-3} mol l_o^{-1}, $f_{10} = 0.875$, $\phi_{w/o} = 0.74$

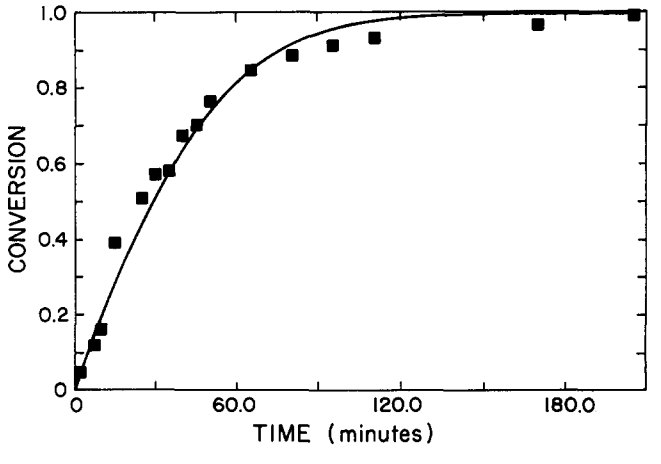

Figure 5 Conversion–time data (■) and kinetic model predictions (———) for an AAM/DMAEM copolymerization at 50°C. Experimental conditions: [monomer] = 6.11 mol l_w^{-1}, [AIBN] = 7.373×10^{-3} mol l_o^{-1}, $f_{10} = 0.875$, $\phi_{w/o} = 0.74$

can be rationalized as follows: Charged macroradicals tend to have less configurational entropy than non-ionic polymers because of the Coulombic interactions that reduce the number of sites on a hypothetical lattice for charged groups to locate. Therefore, chains grow in a more extended form with the radical avoiding the polymer-rich and charge-rich segments of its own and neighbouring chains. Hence, growing chain ends tend to propagate away from the centre of mass and into the solution, where termination reactions would probably not be hindered so much.

Evaluation of the inverse-microsuspension copolymerization kinetic model against experimental data

Figures 4 to *7* show experimental conversion–time data and kinetic model predictions for copolymerizations of AAM with DMAEM at 60, 50 and 40°C, and with DMAEA at 60°C respectively. In all figures, the model is depicted by a full curve and the experimental data by discrete symbols. The kinetic model is observed to give excellent agreement with the experimental observations over all conditions investigated. This validates the generalization of the inverse-microsuspension mechanism to copolymerizations with quaternary ammonium cationic monomers. Specifically, the incorporation of simple copolymerization kinetics within the framework of the inverse-microsuspension mechanism is sufficient for kinetic accuracy. Penultimate influences on propagation, although probably needed to describe the sequence-length distribution, are unnecessary.

Figures 8 and *9* illustrate the magnitude of the composition drift with conversion for copolymerizations of AAM with DMAEM and DMAEA. For comparison, the monomer composition has been predicted using reactivity ratios measured in solution polymerization. The majority of the inverse-microsuspension data lie within the 95% confidence region delineated on the basis of polymerizations in aqueous media. This indicates that the reactivity ratios are not significantly different in inverse microsuspension and solution. The latter, which have been reliably estimated using accurate analytical techniques and unbiased statistical methods[47], can be used in water-in-oil polymerization models. Direct measurements in heterophase systems are not required. Furthermore, the agreement between theoretical and experimental composition drifts gives additional support to the mechanistic assumption of nucleation in the

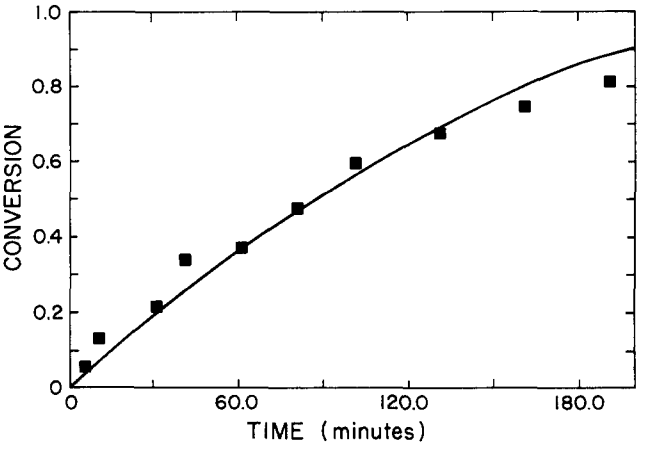

Figure 6 Conversion–time data (■) and kinetic model predictions (———) for an AAM/DMAEM copolymerization at 40°C. Experimental conditions: [monomer] = 6.13 mol l_w^{-1}, [AIBN] = 14.83×10^{-3} mol l_o^{-1}, $f_{10} = 0.877$, $\phi_{w/o} = 0.74$

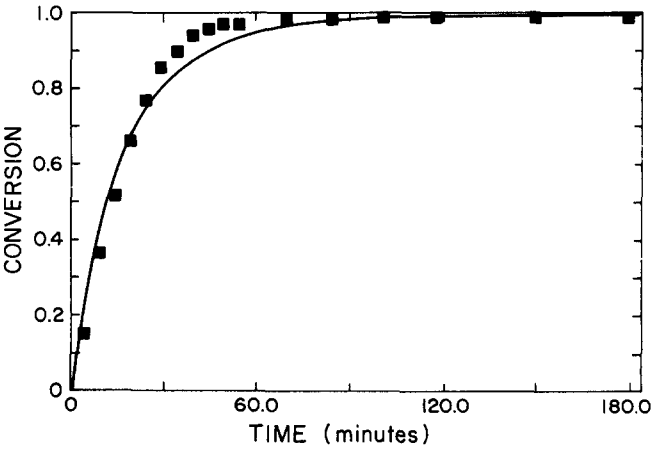

Figure 7 Conversion–time data (■) and kinetic model predictions (———) for an AAM/DMAEA copolymerization at 60°C. Experimental conditions: [monomer] = 6.05 mol l_w^{-1}, [AIBN] = 3.337×10^{-3} mol l_o^{-1}, $f_{10} = 0.840$, $\phi_{w/o} = 0.74$

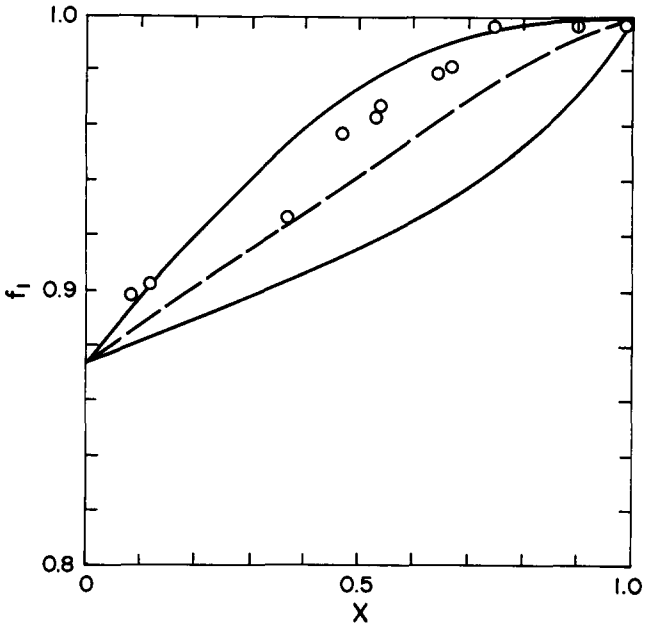

Figure 8 Drift in monomer composition with conversion for an AAM/DMAEM inverse-microsuspension copolymerization at 50°C: (○) experimental data measured by h.p.l.c.; (---) predicted composition based on the reactivity ratios measured in solution polymerization; (———) 95% confidence limits based on the reactivity ratios measured in solution polymerization

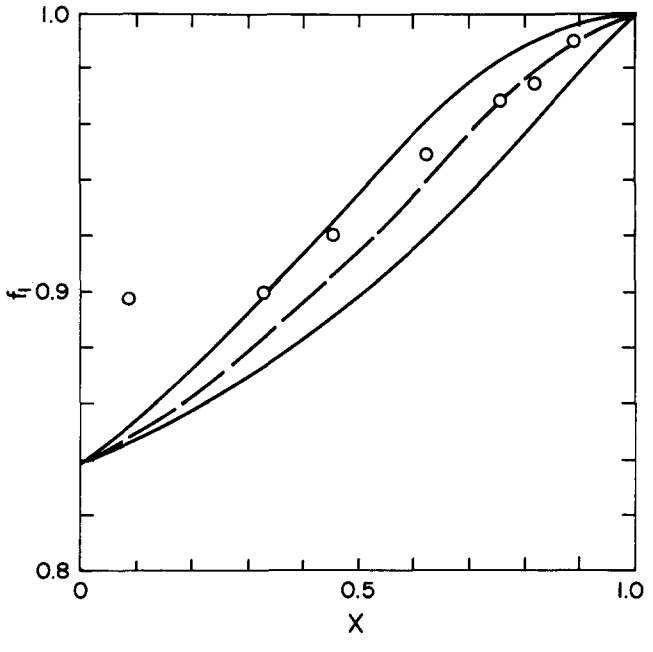

Figure 9 Drift in monomer composition with conversion for an AAM/DMAEA inverse-microsuspension copolymerization at 40°C: (○) experimental data measured by h.p.l.c.; (---) predicted composition based on the reactivity ratios measured in solution polymerization; (———) 95% confidence limits based on the reactivity ratios measured in solution polymerization

monomer droplets. A necessary consequence of this is that each polymer particle behaves like a microbatch solution polymerization reactor, with propagation and termination having the same velocities as in aqueous solution, as has been reported in this paper.

The particle sizes were found to be invariant with conversion. This confirms the model assumption of nucleation in monomer droplets, and is consistent with the trend for acrylamide homopolymerizations[56]. Measurements made by dynamic light scattering and photomicrography gave very similar results, as is shown for an inverse-microsuspension latex in *Figure 10*. The size distribution was quite broad for all samples, as is to be expected for particles produced through a break-up/coalescence mechanism. The volume-average particle size was nominally $7 \pm 1.5\ \mu m$ for all polymerizations. The absence of a thermal dependence is attributed to pre-emulsification and slow agitation speeds.

Figures 11 and *12* simulate the composition drift and initial reaction rate for copolymerizations of AAM with DMAEA and DMAEM respectively. The slower reactivity of the quaternary ammoniums, relative to the

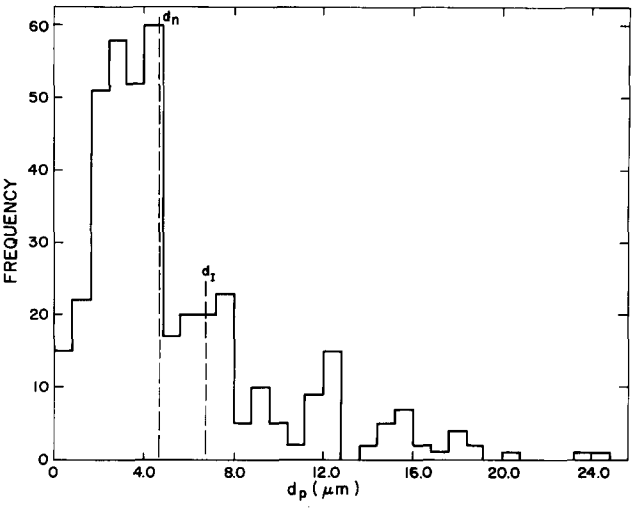

Figure 10 Frequency *versus* diameter (μm) for a particle size distribution of a latex determined by measuring the images from a photomicrograph (*Figure 1A*). The broken vertical lines represent the number (d_n) and intensity (d_I) average particle diameters determined by dynamic light scattering. The sample was withdrawn from a DMAEA polymerization at 60°C. Additional experimental conditions were: [monomer] = 6.05 mol l_w^{-1}, [AIBN] = 3.337×10^{-3} mol l_o^{-1}, $f_{10} = 0.840$, $\phi_{w/o} = 0.74$

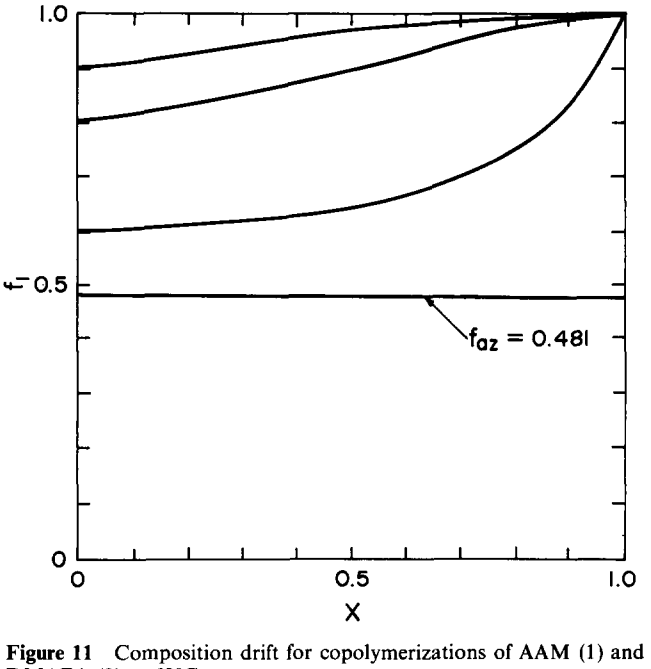

Figure 11 Composition drift for copolymerizations of AAM (1) and DMAEA (2) at 60°C

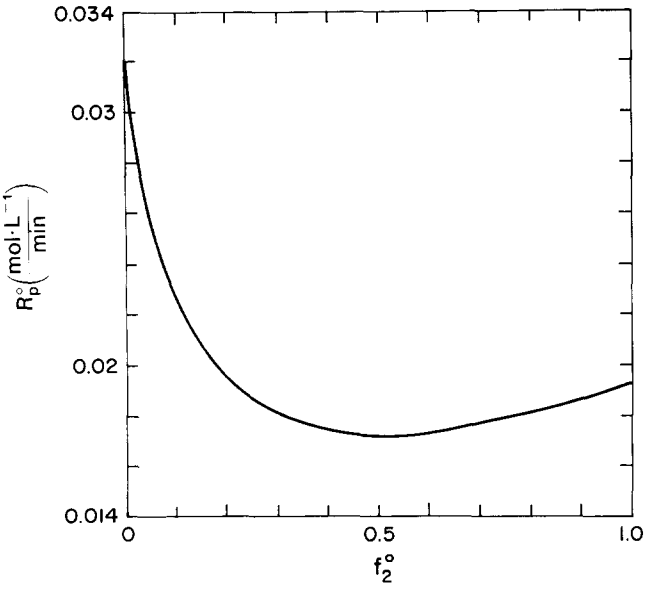

Figure 12 Initial rate of polymerization as a function of comonomer composition. Simulations were performed for an AAM/DMAEM copolymerization at 60°C. The monomer concentration was 0.5 mol l^{-1}. Other conditions were identical to those reported in *Table 3* for these comonomers at the same temperature

non-ionic monomer, results in compositional heterogeneities* (*Figure 12*). These are most acute over the commercial range of copolymer compositions ($F_1 \approx$ 0.9–0.95) (*Figure 11*), and yield a blocky distribution of charge groups along the polymer backbone. This can only be circumvented by eliminating monomer composition drift throughout the polymerization. Continuous processes, semi-batch feed strategies and the utilization of more than one cationic monomer, each with a unique reactivity[66], have all been used successfully to this end.

CONCLUSIONS

An inverse-microsuspension copolymerization mechanism has been developed. This free-radical reaction scheme includes nucleation and polymerization in monomer droplets, heterophase oligoradical precipitation, and unimolecular chain termination with interfacial species. The effect of ionogenic monomers is also explicitly considered. The resulting kinetic model has been evaluated against experimental data for copolymerizations of acrylamide with quaternary ammonium cationic monomers. Good agreement with the rate, copolymer composition and particle characteristics are observed. Supplemental partitioning experiments have confirmed the oligoradical nucleation hypothesis, and found that precipitation is enhanced in direct correspondence to the solubility of the monomer in the organic phase. Homopolymerization and copolymerization experiments have also shown that propagation and termination are unaffected by the nature of the polymerization system, proceeding at equal rates in aqueous solution and inverse microsuspension. The principal kinetic difference between these homogeneous and heterogeneous processes, apart from interfacial termination, is a reduction in the initiation efficiency: water-in-oil polymerizations are characterized by primary radical deactivation in the organic phase and interfacial layer. Based on these observations, a model for the efficiency of initiation in inverse microsuspension is developed. Employing independent estimates of the kinetic and mass-transfer parameters, the initiation model is found to be consistent with experimental polymerization rate data.

* The severity of the compositional inhomogeneity, even at very low conversions, renders molecular-weight measurement methods invalid on these samples. Without such data, the absence of diffusional limitations on bimolecular termination cannot be directly verified

REFERENCES

1 Schuller, W. H., Price, J. A., Moore, S. T. and Thomas, W. M. *J. Chem. Eng. Data* 1959, **4**, 273
2 Klenina, O. V., Fomina, V. I., Klenin, V. I., Avetisyan, P. K., Medvedev, G. P., Klenin, S. I., Bykova, Ye. N. and Milovskaya, Ye. B. *Vysokomol. Soyed.* (*A*) 1984, **26**, 271
3 Panarin, E. F., Solouskii, M. V., Zaikina, N. A. and Afinogenov, G. E. *Makromol. Chem. Suppl.* 1985, **9**, 25
4 Flesher, P., Farrar, D., Hawe, M. and Langley, J. Eur. Pat. 0172723, 1986
5 Orlov, Yu. N., Yegorov, V. V., Gritskova, I. A., Zubov, V. P., Kabanov, V. A. and Pravidnikov, A. N. *Vysokomol. Soyed.* (*A*) 1986, **28**, 493
6 Hammid, S. M. and Sherrington, D. C. *Polymer* 1987, **28**, 325
7 Nagai, K. and Ohishi, Y. *J. Polym. Sci., Polym. Chem. Edn* 1987, **25**, 1
8 Coyner, E. C. US Patent 3026250, 1962
9 Long, E. W. and McCune, H. W. US Patent 3313734, 1967
10 Hoffmann, A. W. *Justus Liebigs Annalen der Chemie* 1861, **145** (Supplement 1), 275
11 Rabinowitz, R., Marcis, R. and Pellon, J. J. *J. Polym. Sci.* (*A*) 1964, **2**, 1233
12 Tsetlin, B. L., Medved, T. Ya., Chiksev, Yu. G., Polikarpov, Ya. M., Rafikov, S. P. and Kabachnik, M. I. *Vysokomol. Soyed.* 1961, **3**, 1117
13 Pellon, J. J. and Valon, K. J. *Chem. Ind.* (*London*) 1964, **32**, 123
14 Bell, G. R. US Patent 3227650, 1966
15 LaCombe, E. M. US Patent 3238276, 1966
16 Marvel, C. S. and Littman, F. R. *J. Am. Chem. Soc.* 1930, **52**, 287
17 Butler, G. B. and Bunch, R. *J. Am. Chem. Soc.* 1949, **71**, 320
18 Butler, G. B. and Ingley, F. L. *J. Am. Chem. Soc.* 1951, **73**, 895
19 Butler, G. B. US Patent 3288770, 1966
20 Staudinger, H. and Heuer, W. *Bericht* 1934, **67**, 1164
21 Butler, G. B. and Angelo, R. J. *J. Am. Chem. Soc.* 1957, **79**, 3128
22 Wandrey, Ch., Jaeger, W., Reinisch, G., Hahn, M., Engelhardt, G., Jancke, H. and Ballschuhi, D. *Acta Polym.* 1981, **32**, 177
23 Butler, G. B. *Acc. Chem. Res.* 1982, **15**, 370
24 Brace, N. O. *J. Polym. Sci.* (*A-1*) 1970, **8**, 2091
25 Brace, N. O. *J. Org. Chem.* 1971, **36**, 3187
26 Lancaster, J. E., Baccei, L. and Panzer, H. P. *J. Polym. Sci., Polym. Lett. Edn* 1976, **14**, 549
27 Ottenbrite, R. M. and Shillady, D. D. 'Polymeric Amines and Ammonium Salts' (Ed. E. J. Goethals), Int. Symp. on Polymeric Amines and Ammonium Salts, Ghent, Belgium, 1979, Pergamon, Oxford, 1980, p. 143
28 Solomon, D. H. and Hawthorne, D. G. *J. Macromol. Sci., Rev. Macromol. Chem.* (*C*) 1976, **15**, 143
29 *Chemical and Engineering News* 1968, **46** (3), 46
30 Winberg, H. E. US Patent 2744130, 1956
31 Nicke, R., Borchers, B. and Tappe, M. *Zellstoff Papier* 1985, **6**, 215
32 Longi, P., Pellino, E., Greco, E. and Mozzocchi, R. *Chem. Ind.* (*Milan*) 1964, **46**, 156
33 Egoyan, R. V., Cabiton, L. M. and Beileryon, N. M. *Armianskii Khim. Zh.* 1979, **32**, 520
34 Egoyan, R. V., Cabiton, L. M. and Beileryon, N. M. *Armianskii Khim. Zh.* 1979, **32**, 93
35 Egoyan, R. V., Cabiton, L. M. and Beileryon, N. M. *Armianskii Khim. Zh.* 1982, **35**, 570
36 Martynenko, A. I., Ruzeiv, R., Wechaeva, A. V., Dzhahilov, A. T., Topchiev, D. A. and Kabanov, V. A. *Uzbeskii Khim. Zh.* 1979, **2**, 59
37 Fujimori, K., Brown, A. S., Costigon, M. J. and Craven, I. E. *Polym. Bull.* 1984, **12**, 349
38 Boothe, J. E., Flock, H. G. and Hoover, M. F. *J. Macromol. Sci., Chem.* (*A*) 1970, **4**, 1419

39 Hahn, M., Jaeger, W. and Reinisch, G. Work Meeting, Chemical Reaction Kinetics, Universitat Leipzig-Section Chimie, 26 Jan. 1984
40 Jaeger, W., Hahn, M., Wandrey, Ch., Seehaus, F. and Reinisch, G. *J. Macromol. Sci., Chem.* (*A*) 1984, **21**, 593
41 Martynenko, A. I., Wandrey, Ch., Jaeger, W., Hahn, H., Topchiev, D. A., Reinisch, G. and Kabanov, V. A. *Acta Polym.* 1985, **36**, 516
42 Topchiev, D. A., Malkandvev, Yu. A., Korshak, Yu. V., Mikitaev, A. K. and Kabanov, V. A. *Acta Polym.* 1985, **36**, 372
43 Wandrey, Ch., Jaeger, W. and Reinisch, G. *Acta Polym.* 1981, **32**, 197, 257
44 Hahn, M., Jaeger, W. and Reinisch, G. *Acta Polym.* 1983, **34**, 322
45 Hahn, M., Jaeger, W., Wandrey, Ch. and Reinisch, G. *Acta Polym.* 1983, **35**, 350
46 Hunkeler, D. and Hamielec, A. E. *Macromolecules* in press
47 Hunkeler, D., Baade, W. and Hamielec, A. E. in 'Polymers in Aqueous Media: Performance Through Association' (Ed. J. E. Glass), American Chemical Society, Washington, DC, 1989
48 Metcalfe, L. D., Martin, R. J. and Schmitz, A. A. *J. Am. Oil Chemists' Soc.* 1966, **43**, 355
49 Kokufuta, E. *Macromolecules* 1979, **12**,351
50 Tanaka, H. *J. Polym. Sci., Polym. Chem. Edn* 1986, **24**, 29
51 Huang, P. C., Singh, P. and Reichert, K.-H. 'Polymer Reaction Engineering' (Eds K.-H. Reichert and W. Geiseler), Huthig and Wepf, New York, 1986, p. 125
52 Wandrey, Ch. and Jaeger, W. *Acta Polym.* 1985, **36**, 100
53 Singh, P., DFG Report 223/13-1, Institut fur Technisch Chemie der Technischen Universitat, Berlin, 1986
54 Yocum, R. H. and Nyquist, E. B. 'Functional Monomers: Preparation, Polymerization and Application', Marcel Dekker, New York, 1973, Vol. 1
55 Boussouira, B. and Ricard, A. *J. Macromol. Sci., Chem.* (*A*) 1987, **24**, 137
56 Hunkeler, D., Hamielec, A. E. and Baade, W. *Polymer* 1989, **30**, 142
57 Baade, W. and Reichert, K.-H. *Eur. Polym. J.* 1984, **20**, 505
58 Vanderhoff, J. W., DiStefanno, F. V., El-Aasser, M. S., O'Leary, R., Schaffer, O. M. and Visioli, D. L. *J. Disp. Sci. Tech.* 1984, **5**, 323
59 Candau, F., Leong, Y. S. and Fitch, R. M. *J. Polym. Sci., Polym. Chem. Edn* 1985, **23**, 193
60 Kurenkov, V. F., Osipova, T. M., Kaznetsov, E. V. and Mygachenkov, V. A. *Vysokomol. Soed.* (*B*) 1978, **20**, 647
61 Dimonie, M. V., Bohina, C. M., Marinescu, N. N., Marinescu, M. M., Cincu, C. I. and Oprescu, C. G. *Eur. Polym. J.* 1982, **18**, 639
62 Hunkeler, D. and Hamielec, A. E. *Macromolecules* in press
63 Gromov, V. F., Galperina, N. I., Osmanov, T. O., Khomikovskii, P. M. and Abkin, A. D. *Eur. Polym. J.* 1980, **16**, 529
64 Srinivason, K. G. Can. Patent 1204535, 1982
65 Easterly, J. P. Jr Eur. Patent 0107226, 1984
66 Becker, L. W. and Larson, E. H. Eur. Patent 0188721, 1986
67 Holzscherer, C., Durrand, J. P. and Candau, F. *Colloid Polym. Sci.* 1987, **265**, 1067
68 Luskin, L. S. in 'Functional Monomers: Their Preparation, Polymerization and Application' (Eds R. H. Yocum and E. B. Nyquist), Marcel Dekker, New York, 1974, Vol. 2
69 Gerduilite, B. Deposited Doc., Viniti 3784417, 1979
70 Katime, I., Nuno, T. and Lorente, L. *Thermochem. Acta* 1985, **91**, 135
71 Kolthoff, I. M. and Miller, I. K. *J. Am. Chem. Soc.* 1951, **73**, 3055
72 Shawki, S. PhD Thesis, McMaster University, 1978
73 Riggs, J. P. and Rodriguez, F. *J. Polym. Sci.* (*A-1*) 1967, **5**, 3151
74 Singh, U. C., Manickam, S. P. and Venkatarao, K. *Makromol. Chem.* 1979, **180**, 589
75 Kim, C. J. and Hamielec, A. E. *Polymer* 1984, **25**, 845
76 Glukhikh, V., Graillat, C. and Pichot, C. *J. Polym. Sci., Polym. Chem. Edn* 1987, **25**, 1127
77 McKechnie, M. T. Conf. on Emulsion Polymers, London, June 1982, Paper No. 3
78 Holtzscherer, C. and Candau, F. *Colloids Surfaces* 1988, **29**, 411